

Technical University of Denmark



Delamination initiated by a defect

Biel, Anders; Toftegaard, Helmuth Langmaack

Published in:
IOP Conference Series: Materials Science and Engineering

Link to article, DOI:
[10.1088/1757-899X/139/1/012015](https://doi.org/10.1088/1757-899X/139/1/012015)

Publication date:
2016

Document Version
Publisher's PDF, also known as Version of record

[Link back to DTU Orbit](#)

Citation (APA):
Biel, A., & Toftegaard, H. L. (2016). Delamination initiated by a defect. IOP Conference Series: Materials Science and Engineering, 139. DOI: 10.1088/1757-899X/139/1/012015

DTU Library

Technical Information Center of Denmark

General rights

Copyright and moral rights for the publications made accessible in the public portal are retained by the authors and/or other copyright owners and it is a condition of accessing publications that users recognise and abide by the legal requirements associated with these rights.

- Users may download and print one copy of any publication from the public portal for the purpose of private study or research.
- You may not further distribute the material or use it for any profit-making activity or commercial gain
- You may freely distribute the URL identifying the publication in the public portal

If you believe that this document breaches copyright please contact us providing details, and we will remove access to the work immediately and investigate your claim.

Delamination initiated by a defect

This content has been downloaded from IOPscience. Please scroll down to see the full text.

2016 IOP Conf. Ser.: Mater. Sci. Eng. 139 012015

(<http://iopscience.iop.org/1757-899X/139/1/012015>)

View [the table of contents for this issue](#), or go to the [journal homepage](#) for more

Download details:

IP Address: 192.38.90.17

This content was downloaded on 13/09/2016 at 09:59

Please note that [terms and conditions apply](#).

You may also be interested in:

[The behavior of delaminations in composite materials - experimental results](#)

A S Chermoshentseva, A M Pokrovskiy and L A Bokhoeva

[Characterization of the Delamination Defects in Marine Steel Using Laser-Induced Breakdown Spectroscopy](#)

Yang Chun, Jia Yunhai, Zhang Yong et al.

[In situ infrared spectroscopic study of cubic boron nitride thin film delamination](#)

Yang Hang-Sheng, Zhang Jian-Ying, Nie An-Min et al.

[Visualization of delamination in composite materials utilizing advanced X-ray imaging techniques](#)

D. Vavrik, J. Jakubek, I. Jandejsek et al.

[Measurement of the Delamination of Thin Silicon and Silicon Carbide Layers by the Multi-Wavelength Laser Ellipsometer](#)

Tohru Hara, Yasuo Kakizaki, Hisao Tanaka et al.

[Finite Element Method Analysis of Nanoscratch Test for the Evaluation of Interface Adhesion Strength in Cu Thin Films on Si Substrate](#)

Atsuko Sekiguchi and Junichi Koike

Delamination initiated by a defect

A Biel and H Toftegaard

Department of Wind Energy, Section of Composites and Materials Mechanics,
Technical University of Denmark, P.O. Box 49, Frederiksborgvej 399, DK-4000
Roskilde, Denmark

abie@dtu.dk

Abstract. Composite materials in wind turbines are mainly joined with adhesives. Adhesive joining is preferable since it distributes the stresses over a larger area. This study shows how a defect can influence the fracture behaviour of adhesively joined composite. Repeated experiments are performed using *double cantilever beam* specimens loaded with bending moments. The specimens consist of two 8 mm thick GFRP-laminates which are joined by a 3 mm thick epoxy adhesive. A thin foil close to one of the laminates is used to start the crack. For some of the specimens a defect is created by an initial load-unload operation. During this operation, a clamp is used in order to prevent crack propagation in the main direction. For the specimens without defect, the crack propagates in the middle of the adhesive layer. For the specimens with defect, the crack directly deviates into the laminate. After about 25 mm propagation in the laminate, the crack returns to the adhesive. Compared to the adhesive the fracture energy for the laminate is significantly higher.

1. Introduction

Manufacturing of large structures, e.g. blades for wind turbines, always include defects. Reduction of defects usually increase the manufacturing costs i.e. it is beneficial to some extent to allow for manufacturing defects. Blades for modern wind turbines are made of adhesively joined composites. A recent study has shown that the adhesive joint at the trailing edge is critical [1]. Accordingly knowledge of how cracks initiate and develops from defects, is essential when designing new structures. Material behavior can be derived from specimens with prefabricated defects.

In the current study we use the *double cantilever beam* specimens (DCB) to determine influence from defects. The specimens have, prior to the main experiment, been exposed to a load-unload operation. The operation creates a visible defect, which influences the result. For comparison, experiments without defects are also performed. A similar experimental procedure has previously been used to determine inelastic properties of an adhesive layers between steel sheets [2,3].

2. Method

The DCB-specimen can be loaded by forces or by moments, see figure 1a. The loads gives a non-uniform stress distribution, see figure 1b. If certain conditions are fulfilled the experiments can be evaluated using the path independent *J*-integral approach [4]. The method has been used in several studies, cf. e.g. [2,5-11]. In order to simplify the experimental setup and the evaluation it is common to load the specimen with either pure forces or pure moments. A short summary of the method is given in the sequel.



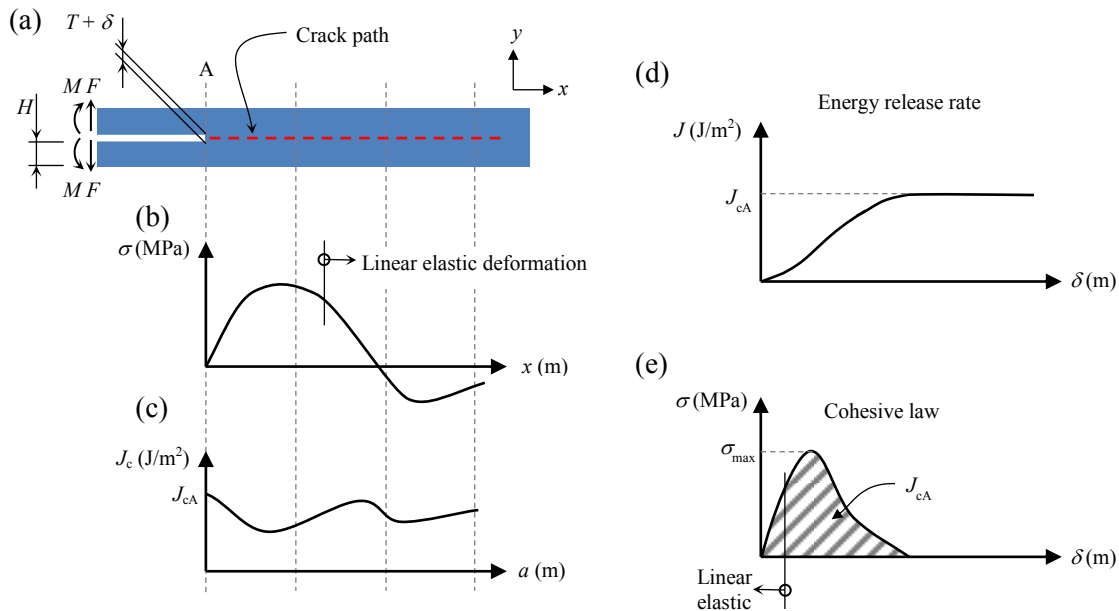


Figure 1. (a) DCB-specimen with used notation, (b) stress distribution along the specimen at beginning of crack propagation, (c) fracture resistance during crack propagation, (d) curve for energy release rate and (e) cohesive laws.

From an external path including the forces and the moments, the *energy release rate* is given by,

$$J = \frac{2F\theta}{B} + \frac{12M^2}{EB^2H^3} \quad (1)$$

where, F is the applied force, θ is the rotation at the loading point, M is the applied bending moment, B is the width of the beam, H is the height of the beam and E is Young's modulus. At crack propagation, the energy release rate equals the fracture energy, e.g. $J = J_c$. The fracture resistance may vary, during the crack propagation, see figure 1c.

By differentiating the energy release rate with respect to a displacement, δ , it is possible to derive the stresses in the beginning of the fracture region, see curves in figure 1d and figure 1e. The stress is given by,

$$\sigma = \frac{\partial J}{\partial \delta} \quad (2)$$

The relation $\sigma(\delta)$ is usually named the *cohesive law*. The cohesive law represents the stress deformation relation of the material. The shape of the cohesive law is dependent on the measurement length T , see figure 1a. Before a macroscopic crack is present, it is common to observe a material softening. For composites, softening can include fibre bridging.

It should be stressed that the method assumes a uniform cohesive law in the loaded region ahead of the crack tip. If the shape of the cohesive law changes along the x -axis, the result using the J -integral approach may be affected [2]. The size of the loaded region is e.g. dependent on the bending stiffness of the beams [8].

3. Specimens and experiments

Twenty-one experiments are performed using three types of specimens. To improve the readability of the paper we introduce three groups, G1, G2 and G3 corresponding to the three types of specimens. The beams of the specimens are made of GFRP-laminates. An insert with a thickness of $12.5\ \mu\text{m}$ is used to create a start for the crack. In order to simplify the manufacturing the insert is attached to one of the beams. Tabs are attached in order to introduce the loads, see figure 2. For two of the groups G1 and G2, the beams are joined with a 3 mm thick epoxy adhesive. Nominally G1 and G2 have the same geometry but for G2 a defect is created by an initial a load-unload operation. For group G3 the adhesive is excluded. The nominal geometry of the specimens are presented in table 1.

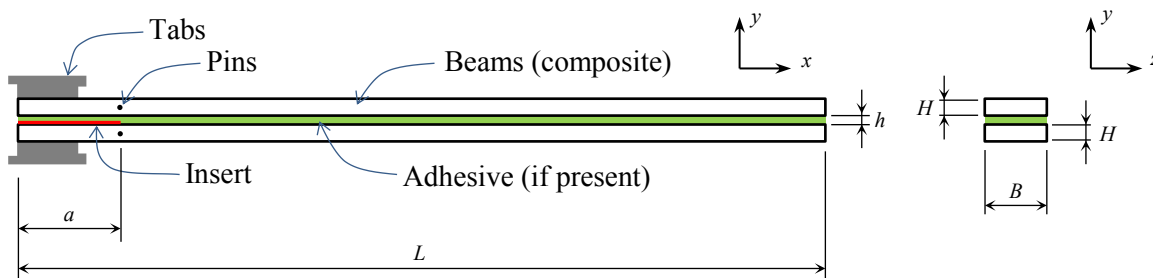


Figure 2. DCB-specimen with used notation

Table 1. Nominal geometry of the used specimens.

Group	Specimens	Defect	H (mm)	h (mm)	B (mm)	a (mm)	L (mm)
G1	8	NO	8	3	30	70	500
G2	7	YES	8	3	30	70	500
G3	6	NO	8	0	30	70	500

The seven specimens in group G2 are exposed to a load-unload operation in order to achieve a defect. During this operation, a clamp with two M8-screws is used in order to prevent main crack propagation, see figure 3a. The load to introduce the defect is applied manually as a moment, see figure 3b. The created defect is visible as small crack across the adhesive, starting from the insert. The direction of the crack is almost perpendicular to the insert. Besides the manually applied load and the loads from the clamping, the direction of the crack may be influenced by residual stresses.

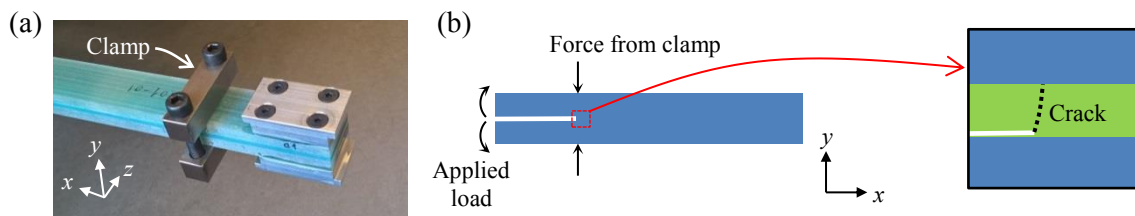


Figure 3. (a) Specimen with applied clamp and (b) forces and crack achieved during the manual load.

By use of a special test frame the DCB-specimens are loaded with pure moments, see figure 4. The setup has been used in several previous studies, cf. e.g. [7,10]. The experiments are loaded quasi statically by constant displacement of the loading point. Each experiment takes about two minutes. The specimen is clamped at the bottom and the moments are applied by use of a wire and two lever arms. The lengths of the lever arms are x_L and x_R . Two load cells are used to measure the force P in the

wire and accordingly the applied moment is, $M \approx P(x_L + x_V)/2$. The separation of the beams δ_{ext} is measured with an extensometer which is applied to the specimens by two pins, see figure 2. Measurement for acoustic emission (AE) and shear deformation (LVDT) is also recorded during the experiments. These data are not used in the present paper.

The main loading is mode I however a slightly mixed mode loading is applied to the crack. As mentioned previously the insert is not placed in the centre of the specimen and there is also a small difference in the length of the lever arms, $x_L = 0.0835$ m and $x_R = 0.0825$ m. All specimens are performed using the same loading conditions. It is presumed that the influence due to mixed mode is minor. A more detailed analyse of mixed mode loading is e.g. given in [12].

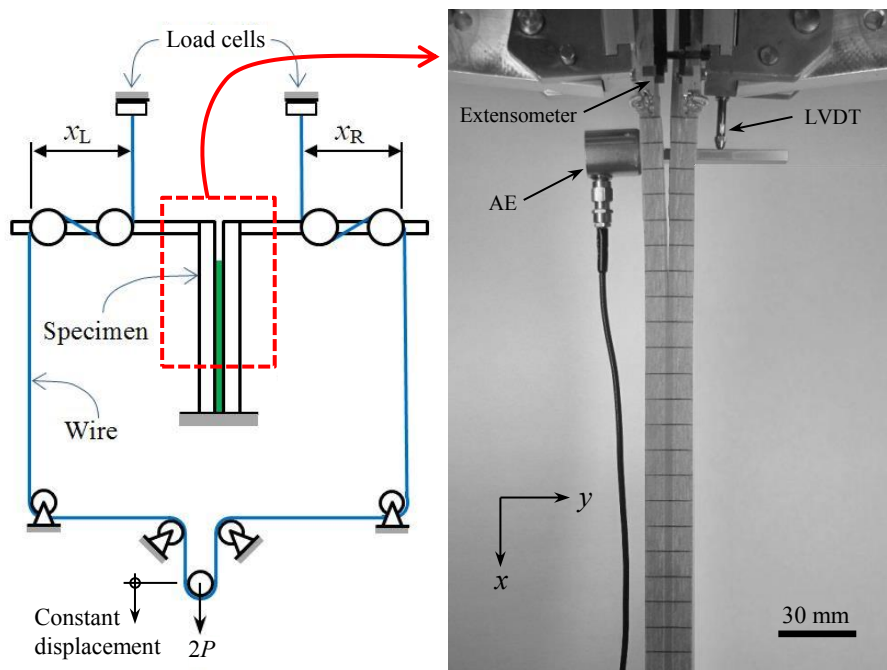


Figure 4. Experimental setup used to load DCB-specimens with pure moments.

4. Results

Significant differences are observed between the three groups. Figure 5a shows the energy release vs. time for all the experiments. The energy release rate is normalized to the average of fracture energy in group G1, J/J_{CG1} . In the beginning, specimens from group G1 and group G2 follow the same curve. For the specimens in group G3 the energy release rate increases faster compared to G1 and G2. The specimens in G3 are stiffer since the adhesive layer is excluded. At, $t \approx 60$ s a deviation is visible between G1 and G2. For the specimens in G1 the energy release rate suddenly drops due to instable crack propagation in the adhesive. Further loading of the specimens in G1 result in a stick-slip crack propagation in the adhesive. For all specimens in G2 except two the energy release rate increase until, $J/J_{CG1} \approx 3.2$. A sudden drop is observed at $t \approx 90$ s. The energy release rates measured after the drop is similar to the ones measured for the stick-slip behaviour in G1. For the specimens in G3 no main drop is observed. The energy release rate increase until, $J/J_{CG1} \approx 2.3$. Figure 5b shows the energy release vs. separation of the beams. For the experiments in G2 and in G3 some deformation is observed before the main crack propagation. For the experiments in G1, no deformation is observed.

Figure 6 shows photos of representative fracture surfaces and sketches of the crack paths for the different groups. For the specimens in G1 a smooth surface is observed. The crack always propagates in the adhesive close to one of the beams. No significant marks from the stick-slip behaviour is visible.

For the specimens in G2 (with defect) the crack starts in the laminate. After a distance about 25 mm the crack enters the adhesive layer. The sudden drop for the specimens in G2 is a result of the crack entering the adhesive layer. No different crack surfaces are observed for the two specimens in G2 which have lower values of the energy release rate. For the specimens in G3 the fracture surfaces are relatively smooth. Some regions with bridging are observed. Compared to the delamination in G2 the fracture surfaces in G3 are smoother.

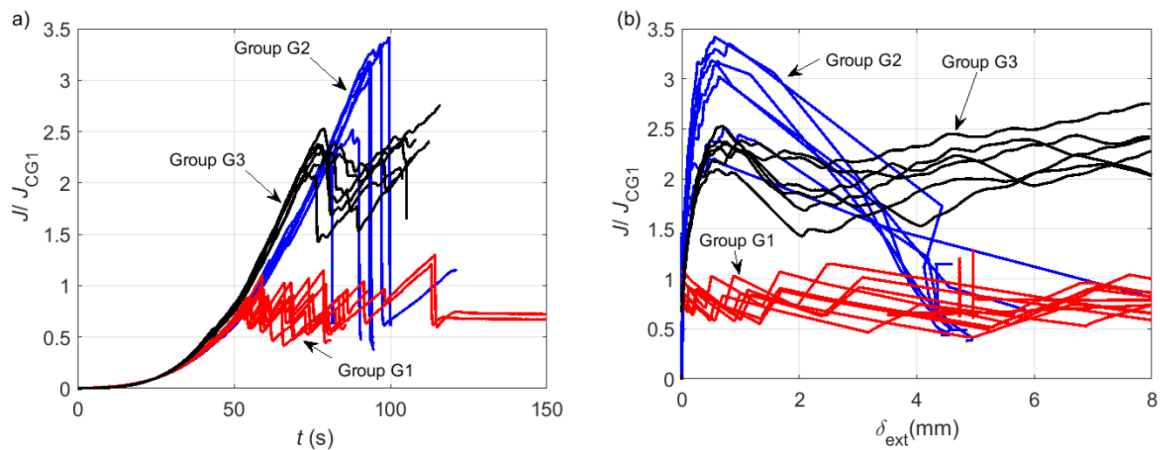


Figure 5. Energy release rate for all experiments (G1, G2, G3) normalized to the average fracture energy for experiments in group G1 vs. (a) time and (b) separation of the beams.

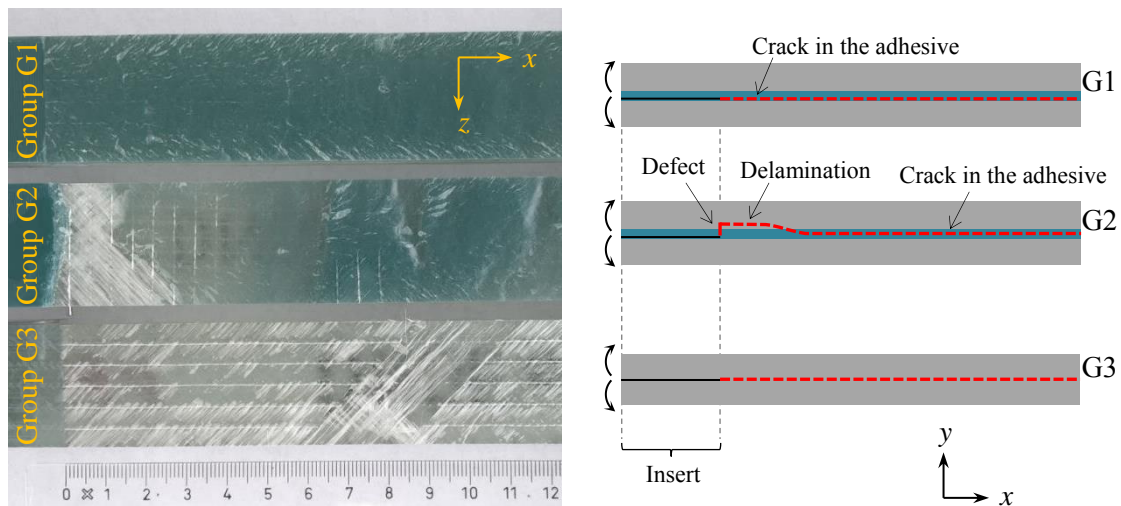


Figure 6. Crack propagation in the specimens; left: Fracture surfaces and right: sketches of the crack paths.

5. Conclusion and discussion

In present paper, it is shown that a defect can change the fracture behavior of a joint. The defect temporarily forces the crack to deviate into the laminate. The fracture resistance of the laminate is significantly higher making it harder to propagate the crack. The defect also increases the instability of the joint. During the crack propagation in the laminate, more elastic energy is stored in the specimen. The energy is suddenly released when the crack enters the adhesive layer.

The result from this study can be used to design new wind turbines. However, some care may be advised. In this paper only one type of defect is analysed. The result will not be valid for all kinds of defects. The used method (J -integral approach) assumes a uniform cohesive law along the specimen. The instable fracture propagation (stick-slip) is an obvious indicator of variations in the cohesive law. To what extent this influences the result is not evaluated.

References

- [1] Eder M and Bitsche R 2015 *Wind Energy* **18** 1007
- [2] Biel A and Stigh U 2010 *Int. J. Fract.* **165** 93
- [3] Biel A and Stigh U 2011 *Procedia Eng.* **10** 2280
- [4] Rice J R 1968 *J. Appl. Mech.* **35** 379
- [5] Paris A J and Paris P C 1988 *Int. J. Fract.* **38** R19
- [6] Suo Z, Bao G and Fan B 1992 *J. Mech. Phys. Solids* **40** 1
- [7] Sørensen B F 2002 *Acta Mat.* **50** 1053
- [8] Andersson T and Biel A 2006 *Int. J. Fract.* **141** 227
- [9] Stigh U, Alfredsson K S, Andersson T, Biel A, Carlberger T and Salomonsson K 2010 *Int. J. Fract.* **165** 149
- [10] Toftegaard H, Rask M, Rasmussen S and Sørensen B F 2013 *6th International Conference on Composites Testing and Model Identification, Department of Mechanical and Manufacturing Engineering, Aalborg University, Denmark* 75
- [11] Marzi S, Rauh A, and Hinterhölzl R M 2014 *Comp Struct* **111** 324
- [12] Sørensen B F, Jørgensen K, Jacobsen T K and Østergaard R C *Int. J. Fract.* **141** 163